

# Bedform transition in a sediment starved environment (SW Baltic Sea)

K. Krämer *Institute of Geosciences, CAU Kiel, Germany – knut.kraemer@ifg.uni-kiel.de*

M. Becker *Institute of Geosciences, CAU Kiel, Germany – marius.becker@ifg.uni-kiel.de*

C. Winter *Institute of Geosciences, CAU Kiel, Germany – christian.winter@ifg.uni-kiel.de*

**ABSTRACT:** The shallow nearshore waters of the southwestern Baltic Sea are a sediment starved environment. Between the wide outer Bay of Kiel and the narrow Fehmarn Belt, a transition from flow parallel sand ribbons through starved dunes into fully developed dunes can be observed. While their general orientation aligns with residual flow pattern, individual dunes exhibit a complex 3D structure. Having been described as dormant, give an estimate of long- and short term migration rates. We also present an approach for measuring starved dune lengths preserving global self-similarity and aspect ratio. The transition from sand ribbons to dunes is linked to the thickness of the mobile sand layer on top of rigid glacial till deposits.

## 1 INTRODUCTION

Lacking sediment input from major rivers, many shallow parts of the western Baltic Sea are considered sediment starved environments (Niedermeyer et al., 2011). The substratum is dominated by till deposits from the last glaciation. This heterogeneous material spanning grain sizes from clay to boulders is reworked and sorted by wave and current action. Mobile sands are available from the erosion of active cliffs (Averes et al., 2021) and abrasion on submarine platforms (Healy, 1980). Larger sand bodies are often confined to the littoral regions and form wave-dominated shore-parallel bars or shore-oblique ridges.

The hydrodynamics of the microtidal western Baltic are governed by fetch-limited waves and wind-induced seiching. Flows generated by basin scale oscillations are channeled through narrow straits, belts and over shallow sills. The Fehmarn Belt is considerably stratified due to the water mass exchange between the North Sea and the Baltic Proper. However, significant inflow of cold, saline and oxygen rich water from the North Sea occurs only during Major Baltic Inflow (MBI) events, which play an important role in hydrodynamics and ecology of the Baltic Sea (Mohrholz et al., 2015).

These limitations in both sediment availability and transport capacity make large flow transverse bedforms a rare phenomenon in this region. Nevertheless, in parts of the narrow straits where both sufficient sediment availability and higher current velocities come together, high energy bedforms such as giant ripples and dunes can be found (Werner & Newton, 1975; Kuijpers et al., 1993) amongst the abundance of other bedforms (Winter et al., this volume).

### 1.1 The bedform field in the southwestern Fehmarn Belt

In the southwestern Fehmarn Belt (FB), a large bedform field extends ca. 8000 m in the main flow direction and ca. 1700 m laterally (Fig. 1a). The bedforms have first been described as asymmetric giant ripples with length of around 60–70 m and heights of around 1.8–2.0 m on the basis of single-beam echosounder recordings (Werner & Newton, 1970). Adapting more recent definitions we use the term dunes to describe the bedforms. Sidescan sonar surveys over larger areas of the Bay of Kiel towards the West show a series of flow parallel sand ribbons which have been proposed exist on lag deposits and serve as conduits feeding sediment into the dune field (Feldens et al., 2015). Investigations including detailed diver observations of individual dune

morphology and fauna distribution found adult specimen of sessile species in the surface layers interpreted as to that the bedforms had been immobile for several years (Werner et al., 1974), leading to the field being described as dormant. Although later studies showed an eastward progression of the eastern boundary, migration rates could not be determined with certainty due to lacking positioning accuracy of the positioning systems used (Feldens et al., 2009, 2015). Advances in GNSS technology and the use of online correction services (RTK) available in nearshore areas now allow for centimeter accuracy in horizontal and vertical domain (Lycourghiotis & Kariotou, 2022). For this study multibeam echosounder (MBES) surveys from recent expeditions were used for the generation of high resolution maps of bedform topography. Precisely positioned grab samples allow for an investigation of sedimentological properties across individual dune geometry and across the transition from sand ribbons to dunes.

## 2 METHODS

### 2.1 Seafloor morphology

Bathymetry and backscatter data were recorded with a MBES (Norbit WBMS STX, 550 kHz, 512 beams at 0.9° width) onboard RV ALKOR during cruises AL536 (05/2020), AL552 (03/2021) and AL574 (06/2022) with typical survey speed of 5 kn, 12 Hz ping frequency and a swath of 120° which in the range of water depths between 15 and 25 m resulted in a beam spacing of roughly 0.2 by 0.15 m across/along-swath. For positioning, a differential GNSS system with online real time kinematic (RTK) corrections was used which allowed a horizontal and vertical position accuracy < 0.02 m. Attitude (heave, pitch and roll) was provided by the build-in motion sensor (Applanix WaveMaster).

The raw MBES data were processed in MB-System (V5.7.9beta26) with corrections for attitude and raytracing using sound velocity profiles from CTD casts. The point cloud data was gridded in 0.5 m resolution to obtain a

digital elevation models (DEM) of bathymetry and beam backscatter intensity.

### 2.2 Sub-bottom profiles

Shallow sub-bottom profiles were recorded in combination with the MBES data with an hull-mounted parametric sub-bottom profiler (Innomar SES-2000® medium, 8/100 kHz).

### 2.3 Sediment samples

Seafloor surface samples were taken by van Veen grab sampler. The position of the samples were recorded using an USBL transponder on the device combined with an RTK GNSS (AL552, 2021) and an RTK GNSS antenna positioned on the A-frame above the wire (AL574, 2022). The position accuracy is estimated as O(1 m) for the USBL and O(0.1 m) for the RTK antenna. In combination with the RTK positioned MBES surveys, this allows for a resolution of elements of the dune morphology (stoss/lee slope, trough) in contrast to the previously used differential GPS positioning which did not allow to differentiate between dune and lag sediments (Feldens et al., 2015). At the time of writing, the samples are being analyzed by dry sieving to obtain grain size distributions.

### 2.4 Hydrodynamics

Flow velocities in the dune field were estimated from a numerical model of the North and Baltic sea (modelling system GETM) available from the COSYNA data web portal (<https://codm.hzg.de/codm/>). Averaged over a representative wind year 09/2016 – 08/2017, the main residual current direction was 99° (Fig. 1b).

### 2.5 Bedform morphology

The dimensions height and length (H, L) of the bedforms were calculated using the 2020 bathymetry. Bed elevation profiles (BEPs) were extracted from the DEM in the main flow direction (99° E) with an along-profile spacing of 0.5 m and a lateral spacing of 10 m between the individual profiles using the Generic Mapping Tools software (GMT V6.0.0, Wessel et al. 2019). The resulting profiles were further

analyzed in GNU Octave (V5.9.0). First, the BEPs were filtered using an (5, 100) m bandpass filter to remove high frequency noise and secondary bedforms as well as the background bathymetry. The resulting zero-mean profiles were evaluated between zero-crossings to find crests as local maxima. As – in the starved state – the space between two dunes can be composed of boulder clay or lag deposits a seemingly random topography unrelated to the dunes and no well-defined troughs may occur (Fig. 2). This environment is challenging for the established methods of separating individual bedforms from BEPs developed for tidal or river dunes (Gutierrez et al., 2018; Cisneros et al., 2020; Wang et al., 2020). Especially the actual lengths of starved bedforms are difficult to obtain. Using crest-to-crest spacing would result in an overestimation of bedform lengths, due to the wide, additional space between individual starved bedforms. Therefore, the first and second maxima in the five-point averaging smoothed curvature were extracted as lee slope end (first peak) and stoss slope onset (second peak). For fully developed dunes, this closely corresponds with the trough location (Fig. 2). Stoss and lee slope lengths and heights were taken as differences in along-profile distance and vertical elevation between those three points. The total dune length was computed as the sum of stoss and lee length and total height as the average of stoss and lee height. Asymmetry was computed from the ratio of stoss and lee length. The resulting bedform dimension parameters were stored and exported for the position of the crest.

Slope angle and direction of the gradient of the bathymetry were calculated from the DEM using GMT `gdgradient`. To identify slipfaces, the resulting DEM was masked with a  $10^\circ$  cutoff. The profiles used for the calculation of the bedform dimensions described above were extracted from the masked DEM. Slipfaces were identified where at least three successive points at the grid spacing of 0.5 m had slopes  $>10^\circ$ . The slipface direction was averaged over the respective segments and exported as vector components towards East and North (Fig. 1a).

## 2.6 Bedform migration rates

To evaluate migration rates a MBES bathymetry from 2007 was compared to data from surveys in 2020, 2021 and 2022. Lacking positioning accuracy, the 2007 was georeferenced with the help of ground control points taken from immobile morphological features in the western part of the survey area. The remaining positioning error is estimated at  $\pm 2$  m. The latest surveys were carried out with RTK GNSS with positioning accuracy below 0.02 m. In a first step, migration rates were estimated manually from the comparison of individual profiles over a few dunes.

## 3 RESULTS

### 3.1 Bedform morphology

Generally, the dune field is separated into an upper terrace in around 14 m water depth and a lower terrace at 21 m (Fig. 1a). The lateral slope between the terraces steepens from West to East. The field is further grouped into at least six distinct trains of dunes. Their origin can be traced to flow parallel sand ribbons curving into Fehmarn Belt from the larger Bay of Kiel towards the East. The individual trains merge laterally but defects and bifurcations along in their merging flanks can be traced for a long distance, in some cases throughout the entire length of the dune field.

Individual dunes show complex 3D geometries with lengthening and increasing planform curvature of crests, bifurcations, and isolated barchanoid dunes. Dune trains traversing the bathymetry gradient at an oblique angle show a behaviour similar to the refraction of shallow water waves: Dune crestlines bend inward when located in greater depth.

The dunes are asymmetric with peaks of  $3^\circ$  and  $13^\circ$  in the distributions of stoss and lee slope angles respectively. The steeper leeward faces dip towards ESE (median  $100^\circ$ ). However, local slipface directions differ across the individual trains from West to East and appear to follow the changing residual flow direction into the FB. Throughout all available surveys starting from SBES in the 70s to recent MBES surveys

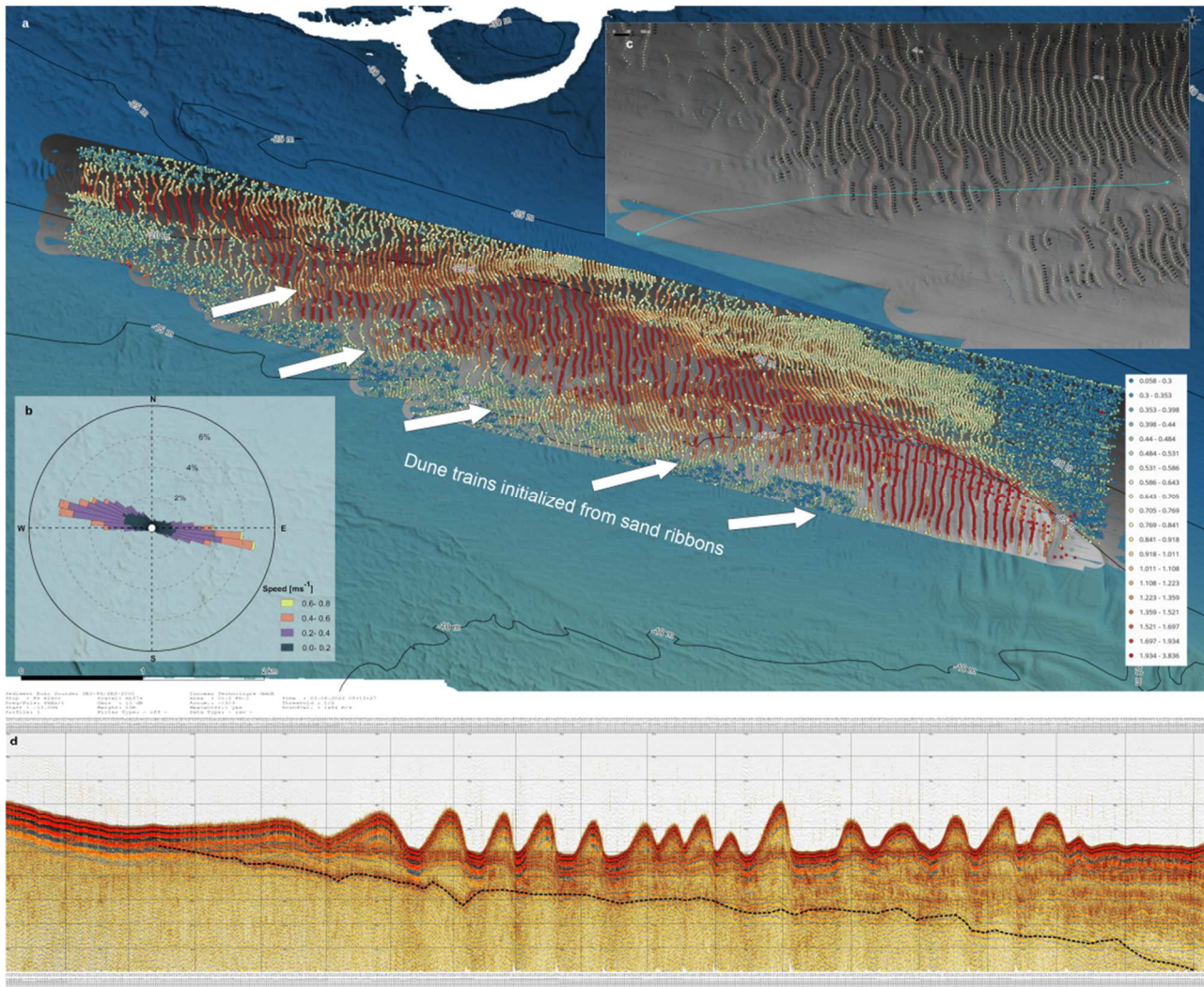


Figure 1. a) Overview map with detected dune crests. Colors indicate dune height. b) Current rose based on a representative wind year 2016/2017. Data: COSYNA. c) Detailed view showing dune topography, detected crests with height and slipface direction vectors for an exemplary transitions of bedform states from flow-parallel sand ribbons over barchanoid forms to starved dunes. The cyan line indicates the track of the SBP profile. d) SBP profile indicating increasing thickness of the mobile sandy bed layer above glacial till deposits (dashed black line).

(2022), a no reversal has not been observed, not even of individual dunes.

### 3.2 Bedform migration rates

Mean long term average migration rates (2007–2020) are estimated to 1.1 m/a. The comparison of the three successive surveys from 05/2020, 03/2021 and 06/2022 showed almost no migration between 2020 and 2021 and migration distances of about 2 m between 2021 and 2022 indicating intermittent dynamics.

### 3.3 Transport layer thickness

A SBP profile which follows the transition from sand ribbons through short-crested barchanoid dunes to starved long-crested dunes shows the increasing thickness of the overlying mobile sand on top of a downward dipping glacial till deposits (Fig. 1d). It is seen that the thickness of the upper sand layer increases from West to East, in general. The highest, most regular and fully developed dunes are found in the shallow eastern part of the bedform field.

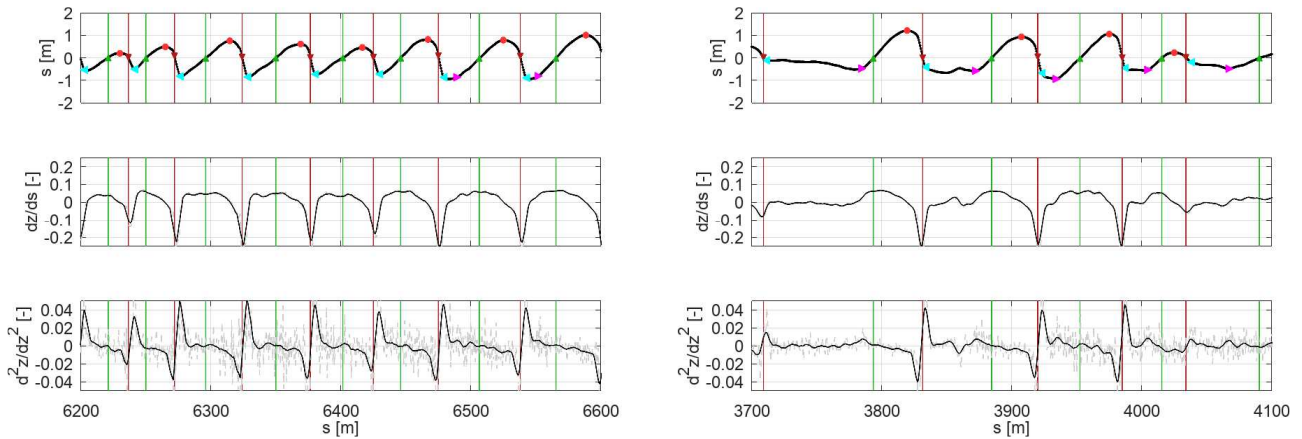


Figure 2. Separation of dunes and measurement of dimensions. Examples for bed elevation profiles  $z(s)$  (top row), slope  $dz/ds$  (middle row) and curvature  $d^2z/ds^2$  (bottom row) for starved dunes (left panels) and fully developed dunes (right panels). Red (down) and green (up) lines mark zero-crossings of the BEPs, red dots mark crest positions, magenta rightward triangles mark stoss slope onset and cyan triangles mark lee slope end.

## 4 DISCUSSION

### 4.1 Determination of starved dune length

In this study a large number of dune shapes (16,372) were analyzed and show a large scatter in height (2<sup>nd</sup> and 98<sup>th</sup> percentiles:  $H_{02} = 0.25$  m,  $H_{98} = 2.14$  m;  $L_{02} = 24.54$  m,  $L_{98} = 109.36$  m). Feldens et al. (2015) stated that the dune steepness “H/L plot beneath the global mean line” of Flemming (1988). This is true when crest to crest distances are used to measure dune length (Fig. 3). When length is measured between first and second curvature peaks as illustrated above and in Fig. 2, H/L ratios of individual dunes plot closer to the global mean given by Flemming (1988) as  $H = 0.0677$   $L_{0.8098}$  (Fig. 3). When the projected length in the direction of the slipface gradient is used in addition, the H/L ratios along individual dunes fit even better.

### 4.2 Planform structure of dunes in relation to local flow and transport pattern

The asymmetric shape of the dunes agrees with the direction of Baltic Sea inflow events, which are possibly the main driver for dune formation and migration. While average slipface directions agree with the main flow direction during inflow events, individual dune crests show a complex 3D structure with both inward focussing and outward fanning which may

locally influence bedload transport directions leading to converging and diverging transport patterns. This potentially influences the sediment supply to the respective downstream dune. Further investigations have to be made into the relation between slipface direction, near-bed flow and bedload transport direction as the latter may be bound to the small scale downslope gradient direction.

### 4.3 Bedform transitions in relation to transport capacity and transport layer thickness

Bedform transitions from sand ribbons to (starved) dunes have to be re-evaluated based on bathymetry and sub-bottom profiles following the sand ribbon and dune train axes. By evaluating transport direction and capacity from high resolution numerical models and determining transport layer thickness of the available mobile sediment above a rigid base layer from SBP profiles the bedform types can be plotted against stability diagrams (e.g. Kleinhans, 2002).

## 5 CONCLUSIONS

In the microtidal southwestern Baltic Sea, a field of starved bedforms is characterized by complex individual geometry and intermittent migration with a long-term average migration rate close to 1.1 m/a. Short term changes in migration rates obtained from annual surveys can help to understand the link between the

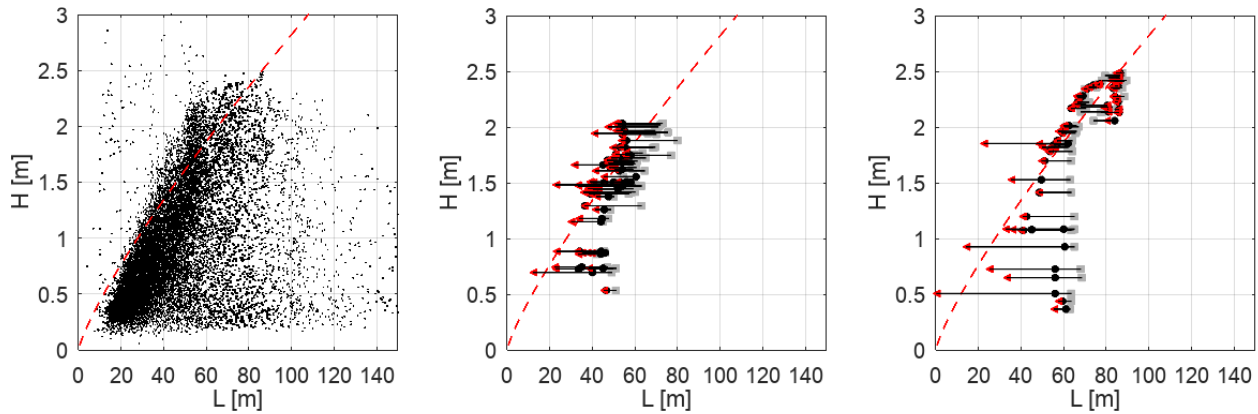


Figure 3. Dune dimensions H, L. The red dashed line indicates the global mean following Flemming (1988). Left: Entire dune field containing 16,372 dune geometries. Middle: Example for a starved dune. Right: Example for a fully developed dune. Grey squares indicate crest-to-crest lengths, black circles indicate adapted length based on first and second BEP curvature peaks and red triangles indicate the additional projection of the curvature-based lengths towards the direction of the corresponding slip faces.

history of forcing events and morphodynamic response of the dunes.

The mode of the bedforms changes from thin flow-parallel sand ribbons to flow-transverse (starved) dunes with the availability of sand from the substratum.

Starved dune lengths can be measured by evaluating local maxima of curvature between crests positions along BEPs. 3D dunes with large crestline curvature should be measured with respect to the direction of the slipface gradient to preserve global self-similarity and aspect ratio, e.g. by defining a curvilinear grid following streamlines for the extraction of the BEPs or by a two-step procedure which first extracts crestlines from parallel BEPs and in a second step follows the crestlines of individual dunes and extracts perpendicular profiles reaching the next upstream and downstream dune.

Porcile et al. (2022) already pointed out the need for further studies to understand the effect of sediment starvation on bedform migration rates. Here, the SW FB dune field could serve as an interesting field site other than spatially constrained river channels or laboratory flumes.

## 6 REFERENCES

- Averes, T., Hofstede, J. L., Hinrichsen, A., Reimers, H. C., & Winter, C. (2021). Cliff retreat contribution to the littoral sediment budget along the baltic sea coastline of Schleswig-Holstein, Germany. *Journal of Marine Science and Engineering*, 9(8), 870.
- Cisneros, J., Best, J., van Dijk, T., Almeida, R. P. D., Amsler, M., Boldt, J., ... & Zhang, Y. (2020). Dunes in the world's big rivers are characterized by low-angle lee-side slopes and a complex shape. *Nature Geoscience*, 13(2), 156-162.
- Feldens, P., Diesing, M., Schwarzer, K., Heinrich, C., & Schlenz, B. (2015). Occurrence of flow parallel and flow transverse bedforms in Fehmarn Belt (SW Baltic Sea) related to the local palaeomorphology. *Geomorphology*, 231, 53-62, 10.1016/j.geomorph.2014.11.021.
- Feldens, P., Schwarzer, K., & Diesing, C. H. M. (2009). Genesis and sediment dynamics of a subaqueous dune field in Fehmarn Belt (south-western Baltic Sea). *Ergebnisse aktueller Küstenforschung*, 80.
- Flemming, B. W. (1988). Zur Klassifikation subaquatischer, strömungstransversaler Transportkörper. *Bochumer geologische und geotechnische Arbeiten*, 29(93-97), 44-47.
- Gutierrez, R. R., Mallma, J. A., Núñez-González, F., Link, O., & Abad, J. D. (2018). Bedforms-ATM, an open source software to analyze the scale-based hierarchies and dimensionality of natural bed forms. *SoftwareX*, 7, 184-189.
- Healy, T. (1980). The efficacy of submarine abrasion vs cliff retreat as a supplier of marine sediment in the Kieler Bucht, western Baltic.
- Kleinans, M. G., Wilbers, A. W. E., De Swaaf, A., & Van Den Berg, J. H. (2002). Sediment supply-limited bedforms in sand-gravel bed rivers. *Journal of sedimentary research*, 72(5), 629-640, 10.1306/030702720629.

- Kuijpers, A., Werner, F., & Rumohr, J. (1993). Sandwaves and other large-scale bedforms as indicators of non-tidal surge currents in the Skagerrak off Northern Denmark. *Marine Geology*, 111(3-4), 209-221.
- Lycourghiotis, S., & Kariotou, F. (2022). The “GPS/GNSS on Boat” Technique for the Determination of the Sea Surface Topography and Geoid: A Critical Review. *Coasts*, 2(4), 323-340.
- Mohrholz, V., Naumann, M., Nausch, G., Krüger, S., & Gräwe, U. (2015). Fresh oxygen for the Baltic Sea—An exceptional saline inflow after a decade of stagnation. *Journal of Marine Systems*, 148, 152-166.
- Niedermeyer, R. O., Lampe, R., Janke, W., Schwarzer, K., Duphorn, K., Kliewe, H., & Werner, F. (2011). Die deutsche Ostseeküste.
- Porcile, G., Damveld, J. H., Roos, P. C., Blondeaux, P., & Colombini, M. (2022). Modelling the Genesis of Sand-Starved Dunes in Steady Currents. *Journal of Geophysical Research: Earth Surface*, e2022JF006796.
- Wang, L., Yu, Q., Zhang, Y., Flemming, B. W., Wang, Y., & Gao, S. (2020). An automated procedure to calculate the morphological parameters of superimposed rhythmic bedforms. *Earth Surface Processes and Landforms*, 45(14), 3496-3509.
- Werner, F., & Newton, R. S. (1970). Riesenrippeln im Fehmarnbelt (westliche Ostsee). *Meyniana*, 20, 83-90.
- Werner, F., & Newton, R. S. (1975). High-energy bedforms in the nontidal great belt linking North Sea and Baltic Sea. In *Geology and Engineering* (pp. 381-389). Academic Press.
- Werner, F., WE, A. & Tauchgruppe Kiel (1974). Sedimentologie und Ökologie eines ruhenden Riesenrippelfeldes. *Meyniana* 26, 39-62.
- Wessel, P., Luis, J. F., Uieda, L., Scharroo, R., Wobbe, F., Smith, W. H., & Tian, D. (2019). The generic mapping tools version 6. *Geochemistry, Geophysics, Geosystems*, 20(11), 5556-5564.

